Quantitative susceptibility mapping of Huntington's disease at 7 Tesla

Clare B Poynton[1], Janine M Lupo[1], Christopher P Hess[1], and Sarah J Nelson[1,2]

[1]*Department of Radiology and Biomedical Imaging, University of California, San Francisco, CA, United States,* [2]*Department of Bioengineering and Therapeutic Sciences, University of California, San Francisco, CA, United States*

Introduction

Huntington's disease (HD) is a genetic disease that causes behavioral, cognitive, and motor dysfunction [1]. HD is caused by abnormal repetition (37 or more repeats) of a CAG sequence in the gene coding for the huntingtin protein. Excessive iron deposition in specific regions of the brain is associated with neurodegenerative disorders that include Huntington's and Parkinson's disease [2]. In vivo quantification of iron may provide insight into its role in pathogenesis and aid in patient diagnosis or monitoring. Iron deposition causes changes in tissue magnetic susceptibility, resulting in measurable changes in the phase of the MR signal that can be modeled as the convolution of a dipole-like kernel and spatial susceptibility distribution. The field-dependent relaxation rate increase (FDRI) has been shown to correlate strongly with postmortem iron [3]. Previous studies have shown differences in FDRI and susceptibility-weighted imaging (SWI) in sub-cortical brain regions of HD patients [1,4], but FDRI requires imaging on two separate scanners, and SWI provides phase-based measurements that are dependent on head orientation and may not correlate as strongly with iron. In this study, we apply the QSM method described in [5] to quantify susceptibility in HD patients and controls imaged at high field (7T).

Theory

Quantifying susceptibility by inversion of a perturbation model (QSIP) has shown strong correlation with postmortem iron [5] and FDRI [6] and is defined in Eq 1. Shim and other low order background fields (i.e. from the torso) are eliminated by calculating the Laplacian of the observed field, $\Delta B = (B_0/3)\, f(\chi)$. The first term in Eq. 1 enforces agreement with the shim-corrected field, where B_0 is the main field strength, $W=|\Delta B|$ is a weighting factor that is thresholded to put more weight on regions of high frequency field shifts; $|\cdot|$ denotes absolute value and $\circ$ denotes Hadamard multiplication. The second term enforces agreement of the estimated and observed field, where M is a brain mask, K is the dipole kernel, and B_e is an estimate of the background field from sources outside the brain (i.e. the skull/sinuses), which is obtained using a co-registered tissue/air susceptibility atlas [5]. In term 3, M^C is a mask of the region outside the brain, and controls how sources outside the brain can vary from the estimate that is produced by the atlas-based modeling.

$$\chi^* = \arg\min_{\chi} \lambda_1 \left| W \circ \left(\Delta B - \frac{B_0}{3} f(\chi) \right) \right|_1 + \lambda_2 \left| M \circ \left(B - \left(K * \chi + B_e \right) \right) \right|_2^2 + \lambda_3 \left| M^C \circ \chi \right|_2^2 \quad [1]$$

where $f = \partial^2/\partial x^2 + \partial^2/\partial y^2 - 2\,\partial^2/\partial z^2$

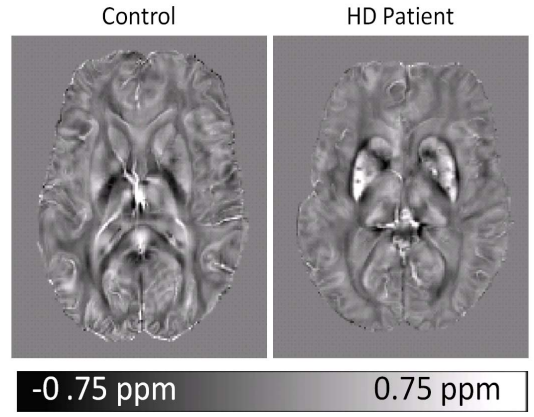

Fig. 1. Comparison of QSM results from a representative HD patient and control shows increased susceptibility values in sub-cortical brain regions.

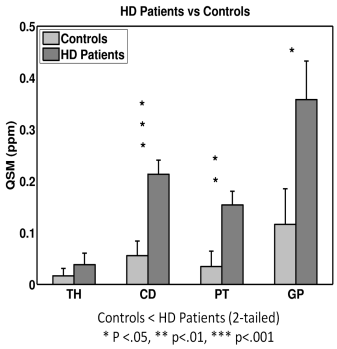

Fig.2. Estimated susceptibility values show statistically significant increases in HD patients, suggesting increased disease-related iron-deposition in these regions.

Methods

Data Acquisition: We analyzed structural MRI and phase data from 12 premotor HD patients (with 40 or more CAG repeats) and 11 age and gender matched controls previously acquired by [4]. All subjects were scanned on 3T and 7T MR scanners (GE Healthcare) with an 8-channel head coil. For phase imaging, 3D SPGR was acquired with TR/TE=80/16 ms, flip angle=20°, FOV=24x24cm^2, and slice thickness=2 mm. To keep the scan time under 6 min, a generalized autocalibrating partially parallel acquisition was used with 3-fold reduction factor, 16 auto calibrating lines, 512x144 acquired matrix, and 0.5x0.5-mm in-plane resolution after zero-filling [7]. T1-weighted images were acquired at 3T, with TR/TE=7/2 ms, flip angle=15°, FOV=23x23 cm^2, matrix=256x256, slice thickness=1 mm, and scan time=6:18 min.
Pre-Processing: Phase maps from each coil were unwrapped [8] and linearly combined using magnitude-squared weighting according to [9]. The magnitude image was computed from the L2 norm of the magnitude data from each channel, and a brain mask was generated from the result using FSL BET [10]. The skull-stripped MNI 152 T1 brain atlas [11] was co-registered to the skull-stripped magnitude image using 12 DOF and normalized mutual information as the cost function; the transform was then applied to the tissue/air susceptibility atlas. *QSM Estimation:* Eq. 1. was solved using standard conjugate gradient techniques to generate QSM maps for each subject in native space. Regions of interest were generated automatically from co-registered T1 data using FSL FIRST [9]. Mean susceptibility (QSM) estimates were computed in four brain regions: caudate (CD), putamen (PT), globus pallidus (GP), and thalamus (TH), and group averages for each region were computed. QSM maps for a representative HD patient and control were registered non-linearly to the SRI atlas [12] using FSL FNIRT [10] for visualization purposes.

Results

QSM results computed from 7T phase data showed increased susceptibility values in all four sub-cortical regions in HD patients relative to controls (Fig. 1). Statistically significant differences were seen in CD, PT, and GP, with CD showing the most significant difference (Fig. 2). This is consistent with FDRI results in HD patients [1]. These results suggest that QSM may allow HD-related iron deposition to be estimated in-vivo using phase data acquired at 7T from standard GRE sequences, which could have important implications for patient identification, stratification and monitoring.

References: [1] Bartzokis G, et al. Neurochem Res, 2007, 32:1655-1664. [2] Chen JC, et al. AJNR Am J Neuroradiol, 1993, 14(2):275-81. [3] Pfefferbaum et al. NeuroImage, 2009, 47(2):493-500. [4] Apple A, et al. AJNR Am J Neuroradiol (in submission). [5] Poynton C, et al. ISMRM, 2012, #6166. [6] Poynton C, et al. IEEE TMI (in submission). [7] Lupo JM, et al. MRI, 2009, 27(4):480-8. [8] Cline H, et al. MRM, 2004, 51(6):1129-37. [9] Bernstein, MA, et al. MRM, 1994, 32:330-334. [10] http://www.fmrib.ox.ac.uk/fsl/ [11] Fonov V, el al. NeuroImage, 2011, 54(1):313-27. [12] Rohlfing T. Hum Brain Mapp, 2010, 31(5):798-819.
Acknowledgements: UC Discovery Grant, ITL-BIO 04-10148, an academic industry partnership grant with GE Healthcare.